

Supplementary materials for:

Synthesis and *in silico* modelling of the potential dual mechanistic activity of small cationic peptides potentiating the antibiotic novobiocin against susceptible and multi-drug resistant *Escherichia coli*

Ilaria Passarini¹, Pedro Ernesto de Resende², Sarah Soares², Tadeh Tahmasi¹, Paul Stapleton², John Malkinson², Mire Zloh^{1,3*} and Sharon Rossiter^{1*}

¹ School of Life and Medical Sciences, University of Hertfordshire, College Lane, Hatfield, AL10 9AB, UK; i.passarini@herts.ac.uk (I.P.), tadehtahmasi@gmail.com (T.T.), zloh@live.co.uk (M.Z.), s.rossiter@herts.ac.uk (S.R.).

² UCL School of Pharmacy, 29-39 Brunswick Square, London WC1N 1AX, UK; pedroderesende@gmail.com (P.R.), sarahapso@gmail.com (S.S.), p.stapleton@ucl.ac.uk (P.S.), j.malkinson@ucl.ac.uk (J.M.).

³ NanoPuzzle Medicines Design, Stevenage, UK; zloh@live.co.uk

* Correspondence: s.rossiter@herts.ac.uk (S.R.), zloh@live.co.uk (M.Z.)

Contents

1. HPLC data for purified peptides	2
2. Mass spectrometry	10
3. NMR data	12
4. Biological assays.....	14
5. MD simulation and docking studies.	16
6. Docking against RND efflux pump as a target.....	18

1. HPLC data for purified peptides

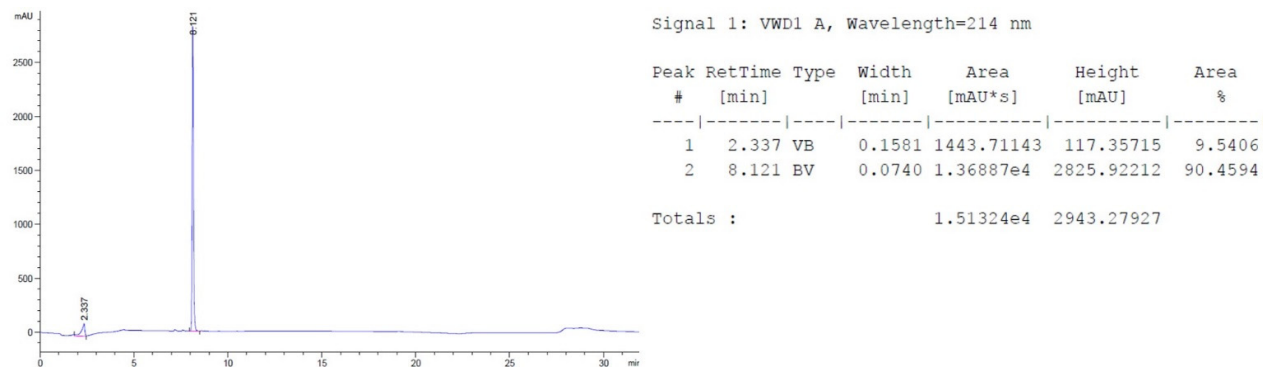


Figure S1 Analytical chromatogram of peptide **1** FRW after purification

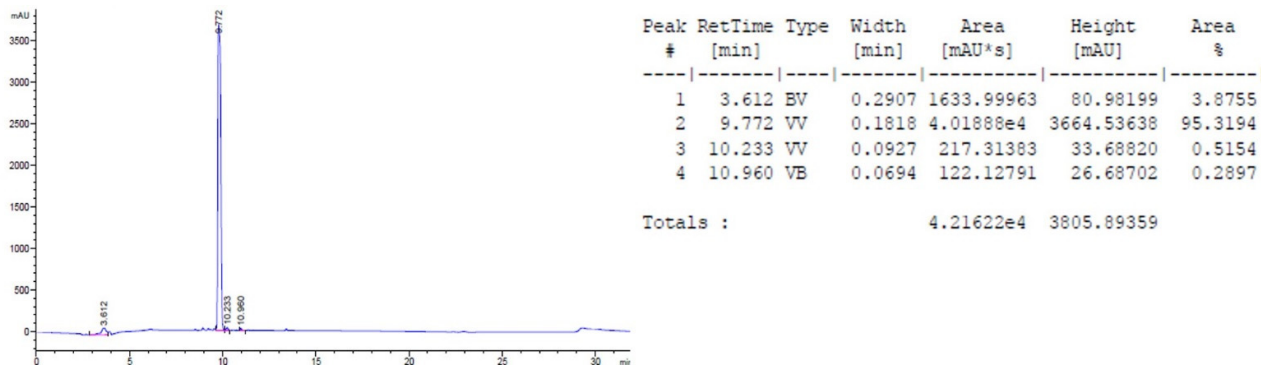


Figure S2. Analytical chromatogram of peptide **2** FWR after purification

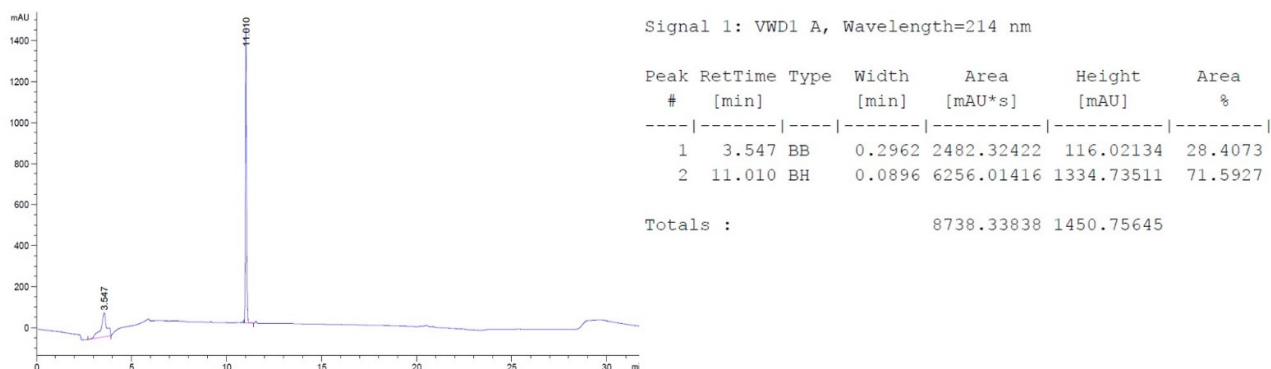


Figure S3. Analytical chromatogram of peptide **3** WRW after purification

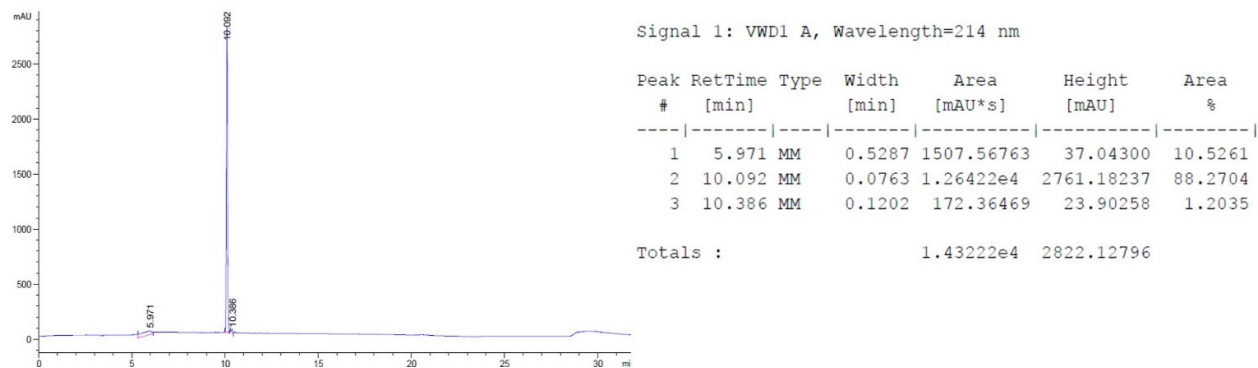


Figure S4. Analytical chromatogram of peptide 4 WRWR after purification

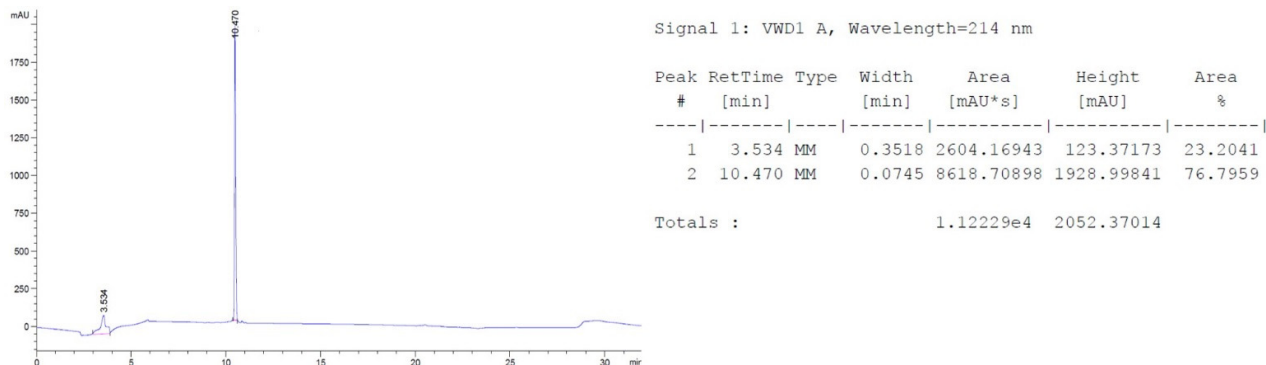


Figure S5. Analytical chromatogram of peptide 5 RWRW after purification

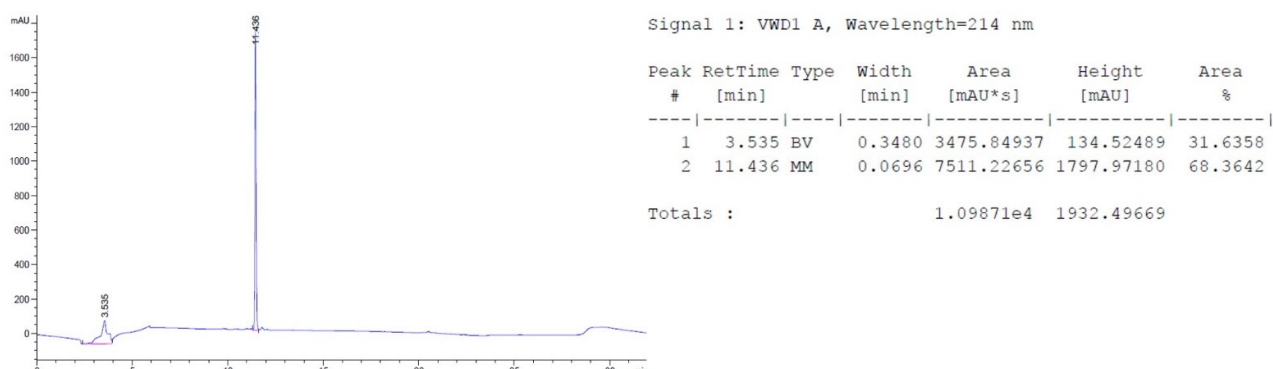


Figure S6. Analytical chromatogram of peptide 6 WRWRW after purification

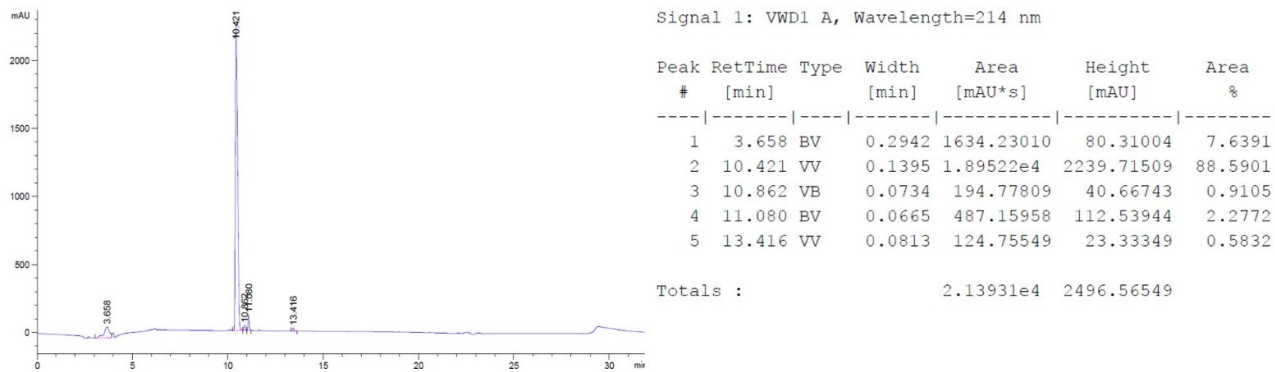


Figure S7. Analytical chromatogram of peptide 7 FRF after purification

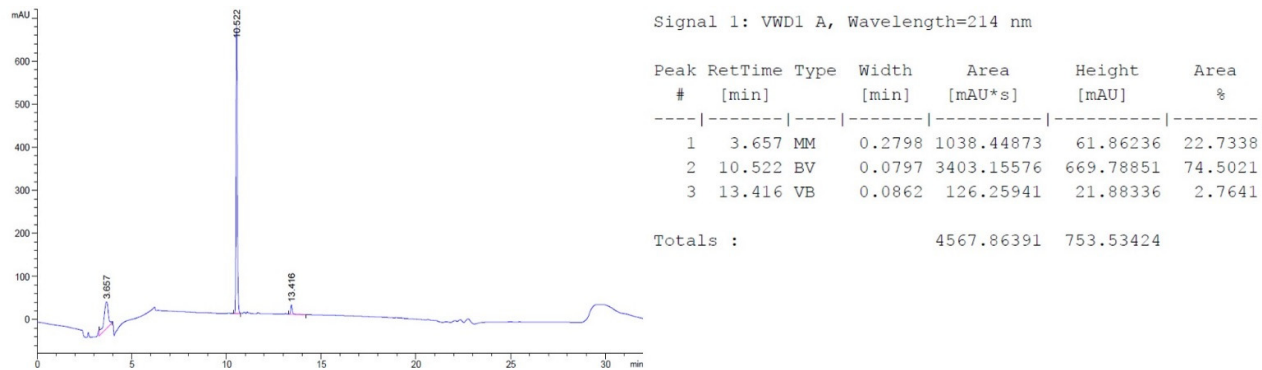


Figure S8. Analytical chromatogram of peptide 8 FRFR after purification

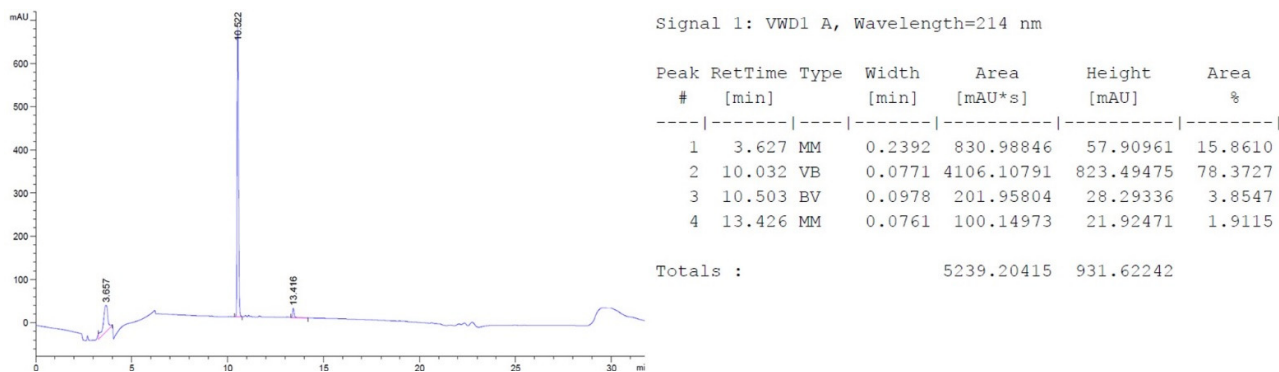


Figure S9. Analytical chromatogram of peptide 9 RFRF after purification

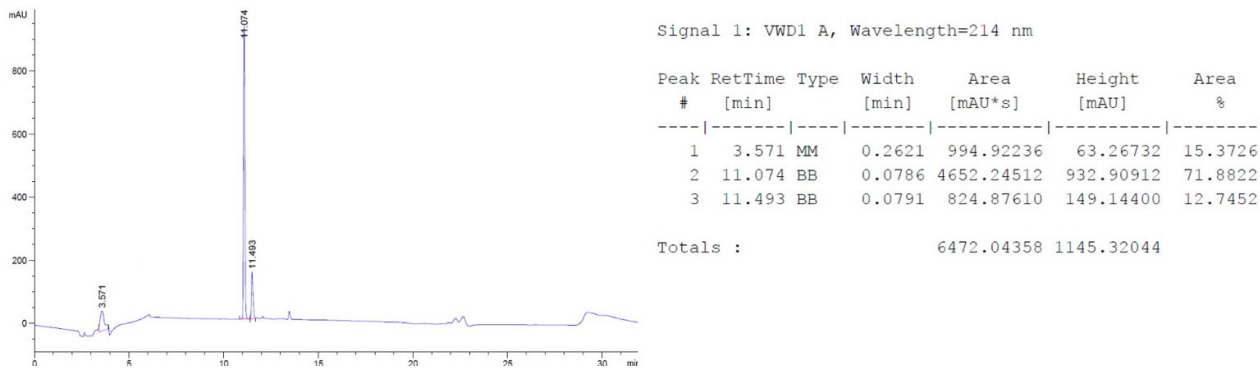


Figure S10. Analytical chromatogram of peptide **10** FRFRF after purification

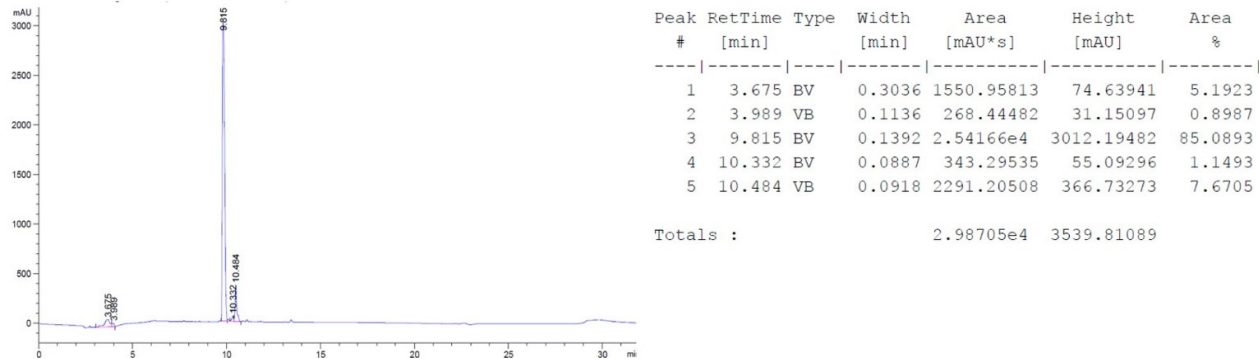


Figure S11. Analytical chromatogram of peptide **11** RRFRF after purification

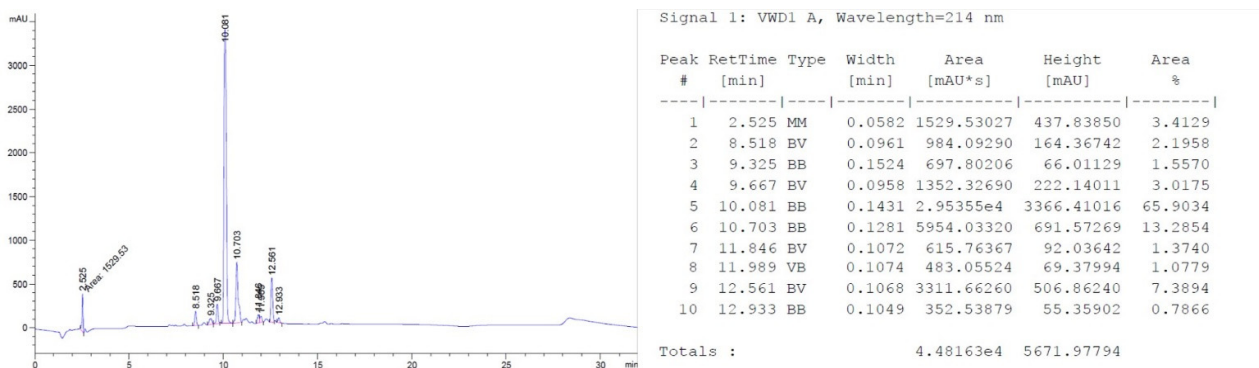


Figure S12. Analytical chromatogram of peptide **12** WKW after purification

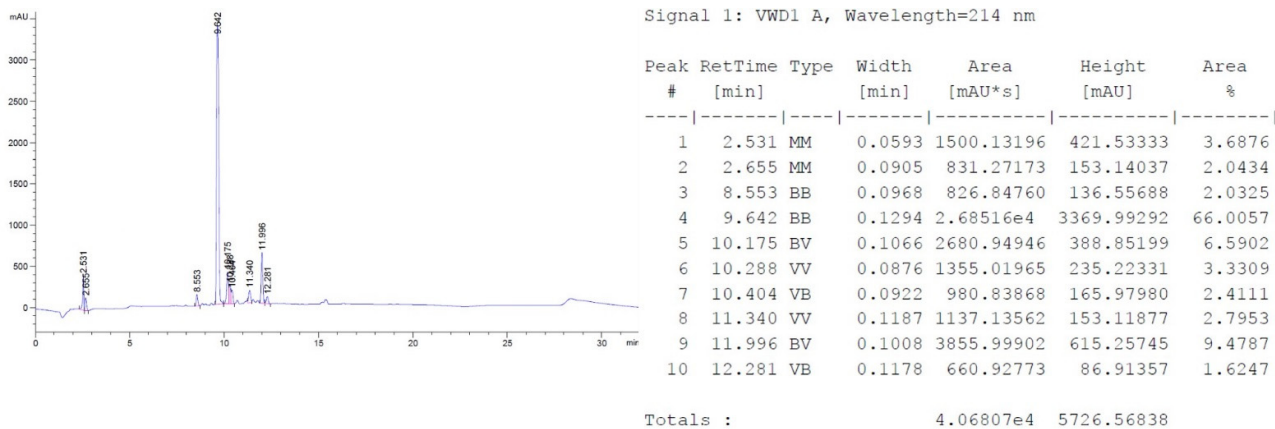


Figure S13. Analytical chromatogram of peptide **13** WKWK after purification

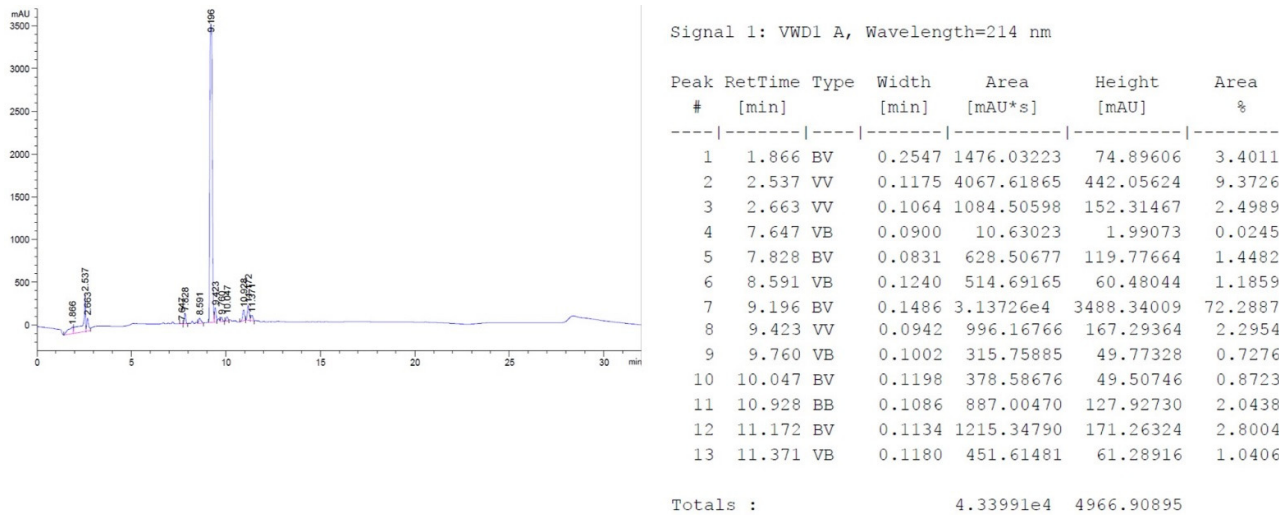


Figure S14. Analytical chromatogram of peptide **14** KWKW after purification

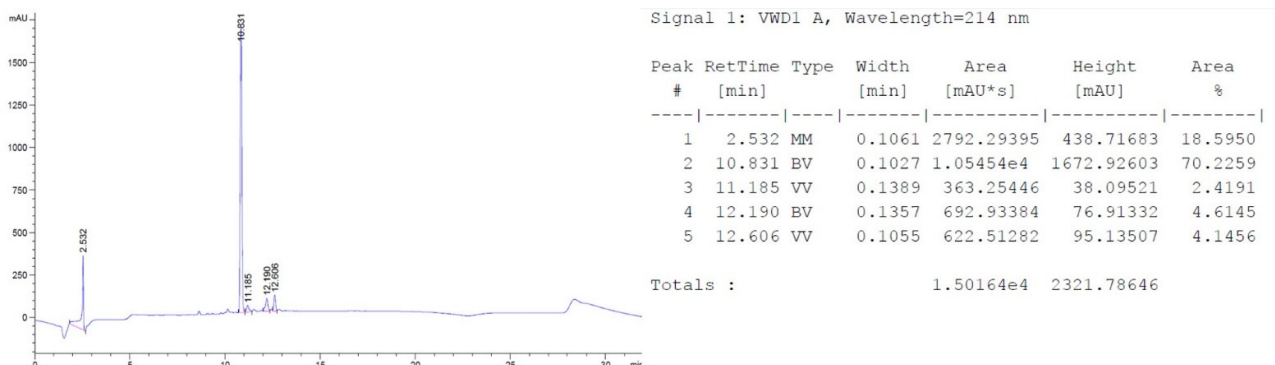


Figure S15. Analytical chromatogram of peptide **15** WKWKW after purification

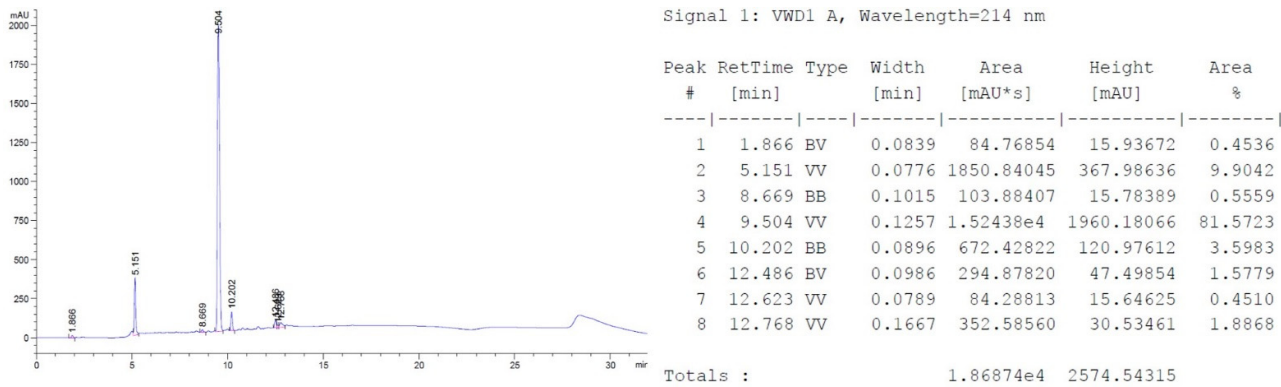


Figure S16. Analytical chromatogram of peptide **16** FKF after purification

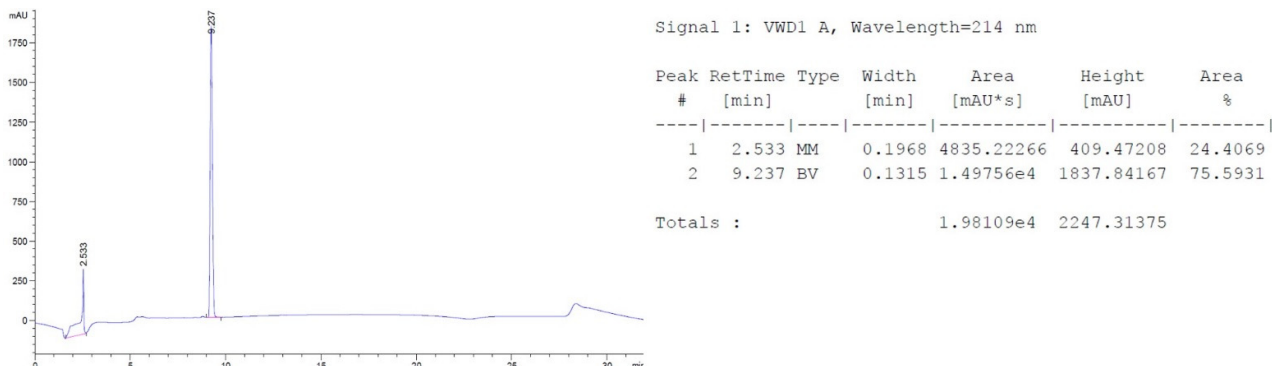


Figure S17. Analytical chromatogram of peptide **17** FKKF after purification

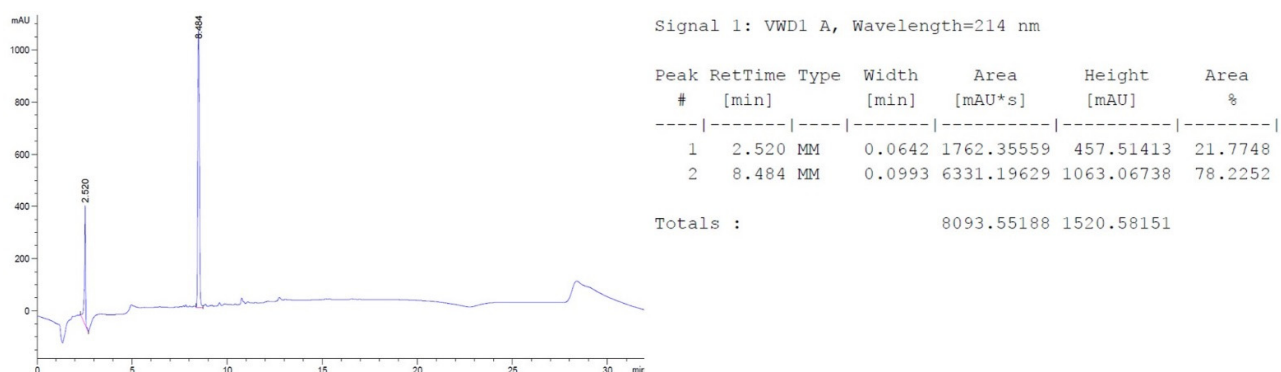


Figure S18. Analytical chromatogram of peptide **18** KFKF after purification

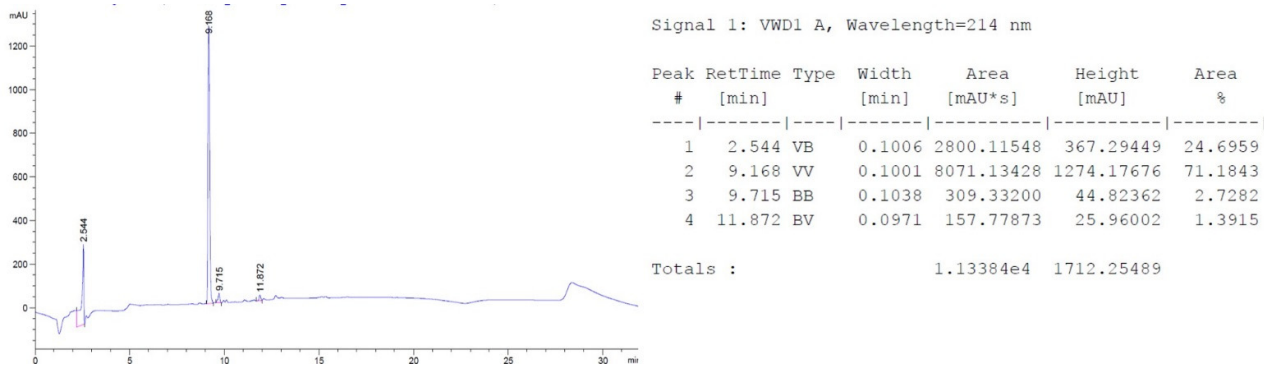


Figure S19. Analytical chromatogram of peptide **19** FKFKF after purification

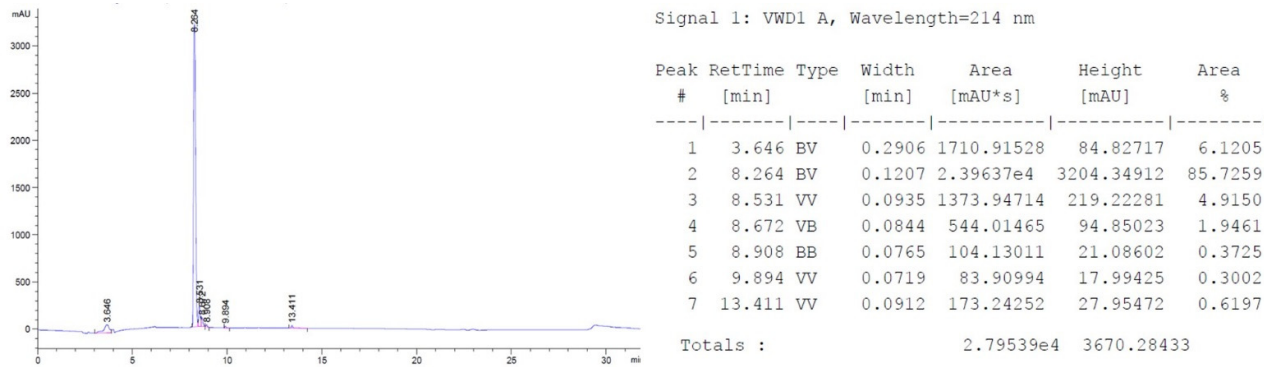


Figure S20. Analytical chromatogram of peptide **22** RPRPRPL after purification

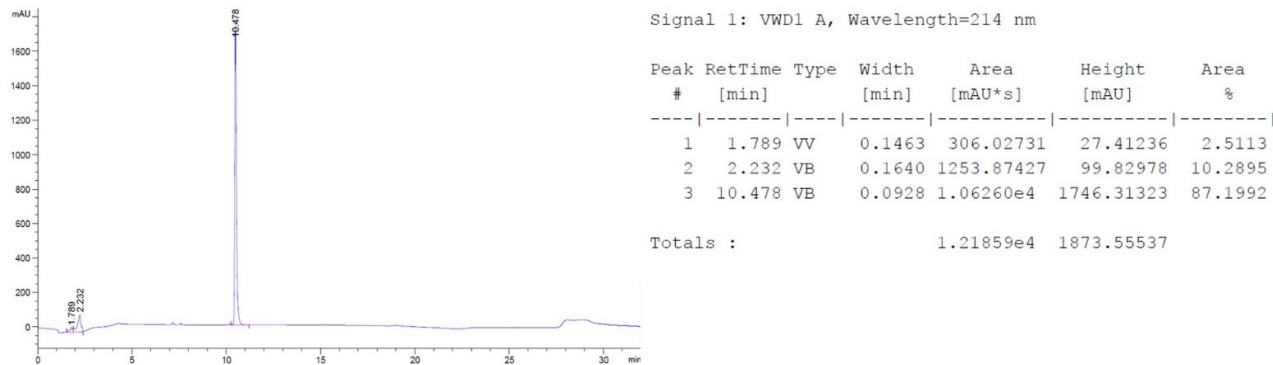


Figure S21. Analytical chromatogram of peptide **23** RPWPPR after purification

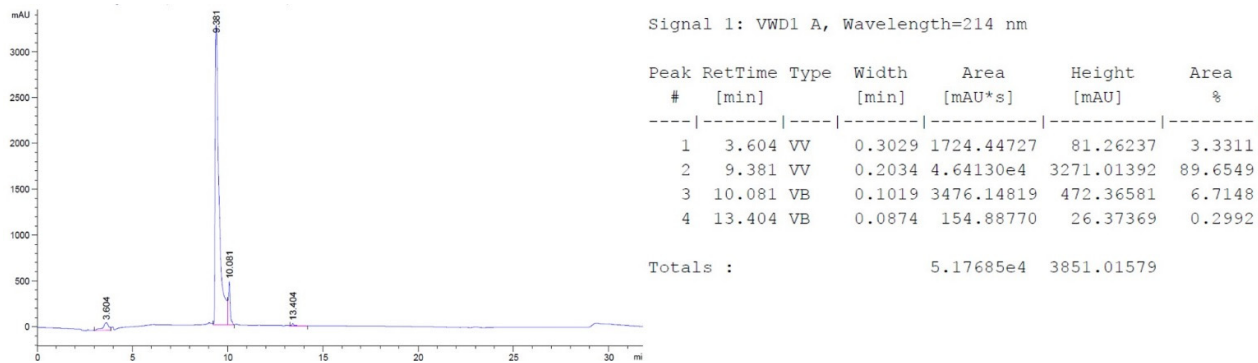


Figure S22. Analytical chromatogram of peptide **24** WKPLPPR after purification

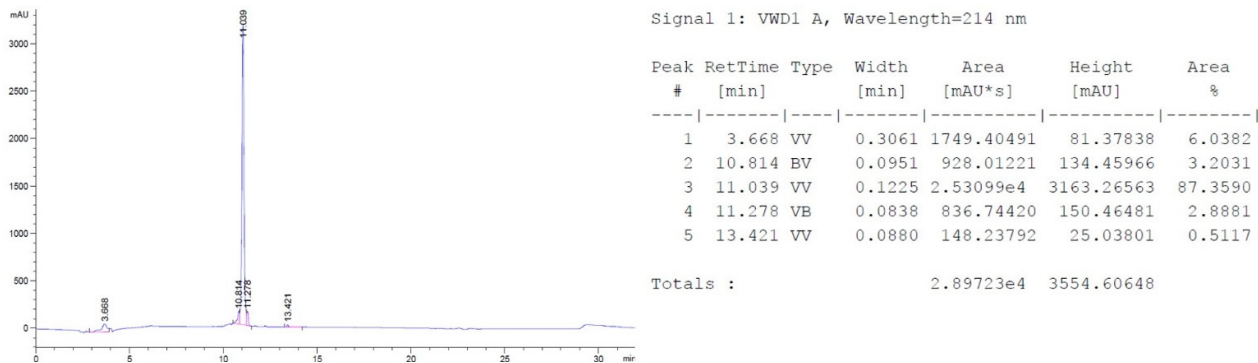


Figure S23. Analytical chromatogram of peptide **26** RPPWRPPW after purification

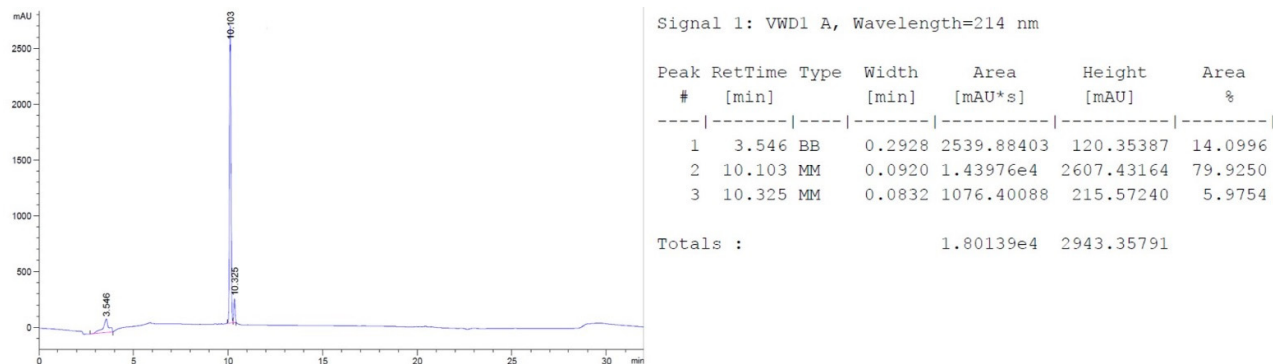


Figure S24. Analytical chromatogram of peptide **27** RP RR PRLPW after purification

2. Mass spectrometry

Synthesised peptides were further characterised through mass spectrometry (LC-MS) (Table S2). Total ion chromatograms were obtained on a Varian Prostar triple-quad LC-MS with integrated ESI detector. All pure samples were initially dissolved in 0.02% v/v trifluoroacetic acid in water and were then eluted through a C18-2 5 μ m, 250x4.6 mm TemesilTM HPLC column. A mixture of 0.1% v/v formic acid in water (solvent A) and 0.1% v/v formic acid in acetonitrile (solvent B) was used as mobile phase with the following gradient: 10% to 90% B over 20 minutes, maintain 90% B for 5 minutes and then back at 10% B over 7 minutes, with flow rate set at 1 mL/min. The mass of the main peak corresponding to the molecular ion was confirmed with a Varian triple-quad mass spectrometer integrated with ESI detector with voltage capillary set at 80.000 V.

Table S1. *m/z* ratios and LC-MS retention times of synthesised peptides

	Sequence	Molecular mass / amu	Basic residue s	Elution time / min	Observed <i>m/z</i> (100% abundance unless stated)
1	FRW	506.3	1	6.60	507.4 [M + H] ⁺
2	FWR	506.3	1	5.48	507.3 [M + H] ⁺
3	WRW	545.3	1	6.91	546.3 [M + H] ⁺
4	WRWR	701.4	2	5.42	351.8, [M + 2H] ²⁺ , 702.4, 7%, [M + H] ⁺
5	RWRW	701.4	2	5.85	351.9 [M + 2H] ²⁺
6	WRWRW	887.5	2	7.16	444.9 [M + 2H] ²⁺
7	FRF	467.3	1	6.18	468.4 [M + H] ⁺
8	FRFR	623.4	2	4.75	312.8 [M + 2H] ²⁺
9	RFRF	623.4	2	5.11	312.8 [M + 2H] ²⁺ , 624.4, 40% [M + H] ⁺
10	FRFRF	770.4	2	7.11	386.5 [M + 2H] ²⁺
11	RRFRF	779.5	3	4.75	261.4, [M + 3H] ³⁺ , 391.4, [M + 2H] ²⁺
12	WKW	517.3	1	6.75	518.30 [M + H] ⁺
13	WKWK	645.4	2	5.35	323.5 [M + 2H] ²⁺ , 646.5, 20% [M + H] ⁺
14	KWKW	645.4	2	5.83	324.0 [M + 2H] ²⁺
15	W WKW	831.5	2	6.98	417.0 [M + 2H] ²⁺
16	FKF	439.3	1	6.14	440.2 [M + H] ⁺
17	FKFK	567.4	2	4.48	285.0 [M + 2H] ²⁺ , 568.5, 15% [M + H] ⁺
18	KFKF	567.4	2	5.19	284.9 [M + 2H] ²⁺ , 568.5, 35% [M + H] ⁺
19	FKFKF	714.4	2	6.56	358.5 [M + 2H] ²⁺ , 715.7, 10% [M + H] ⁺
22	RPRPRPL	889.6	3	3.06	297.8 [M + 3H] ³⁺
23	RPWPPR	806.5	2	4.83	404.5 [M + 2H] ²⁺
24	WKPLPPR	891.5	2	5.10	447.30 [M + 2H] ²⁺ , 892.7, 10% [M + H] ⁺
26	RPPWRPP W	1089.6	2	7.13	546.0 [M + 2H] ²⁺
27	RPRRPRLP W	1231.8	4	4.93	411.7 [M + 3H] ³⁺ , 617.0, 35% [M + 2H] ²⁺

3. NMR data

Peptides **6** and **27** were selected for further investigation and were analysed using NMR spectroscopy, to confirm the expected sequence and connectivity of the residues (Figures S27 and 28; Tables S6 and S7).

¹H, NOESY and TOCSY NMR were acquired in a 10% v/v D₂O solution in water on a Bruker Avance 500 MHz spectrometer.

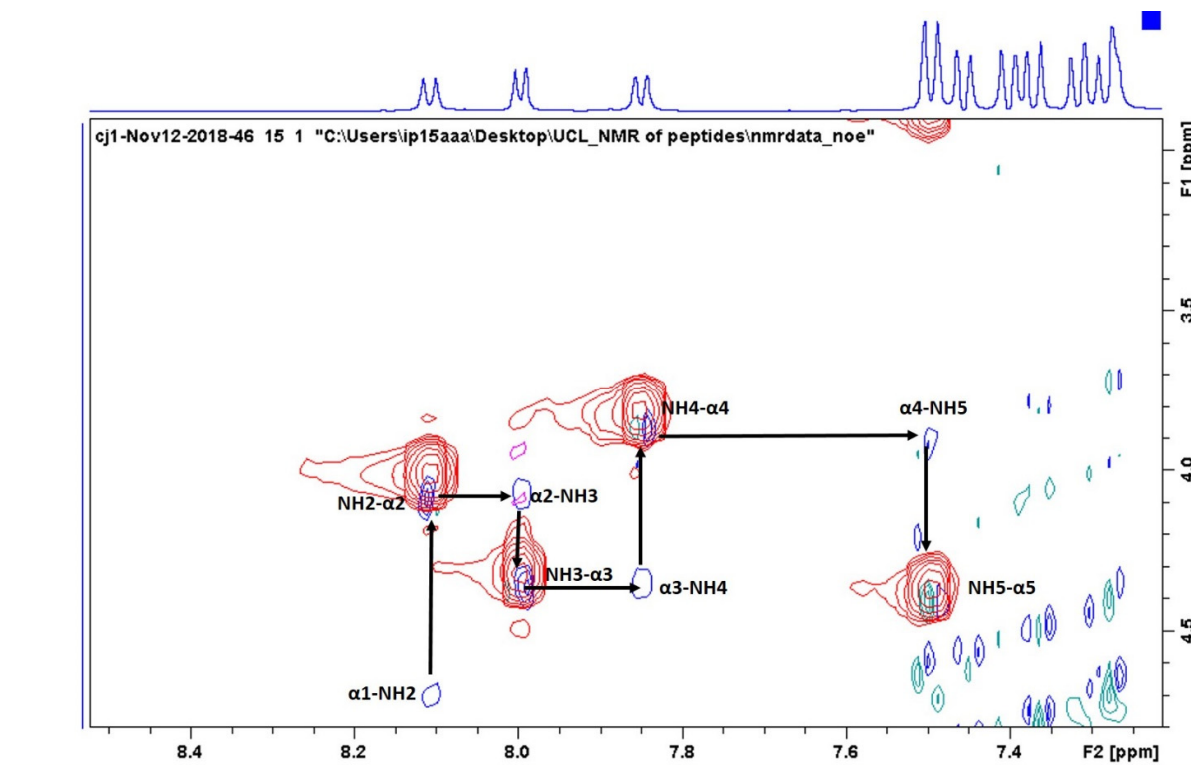


Figure S25. Overlay of the aromatic regions obtained from 2D ¹H-¹H TOCSY (red) and NOESY (blue) NMR spectra of peptide **6** (WRWRW), with relevant connectivity indicated by black arrows.

Table S2. Assignments of ¹H NMR spectra of peptide **6** (WRWRW) based on the overlapping of 2D ¹H-¹H TOCSY and NOESY spectra.

Residue	H- $\text{N}\alpha$	H- α	H- β	H- γ	H- δ	Other
Trp1		4.72				6.95-7.45 (Ar) 10.9 (N α H)
Arg2	8.10	4.01	1.47; 1.40	1.24	2.55	
Trp3	7.99	4.33	2.61			6.95-7.45 (Ar) 10.9 (N α H)
Arg4	7.84	3.80	1.36; 1.30	1.05	2.43	
Trp5	7.51	4.39	2.86; 2.63			6.95-7.45 (Ar) 10.9 (N α H)

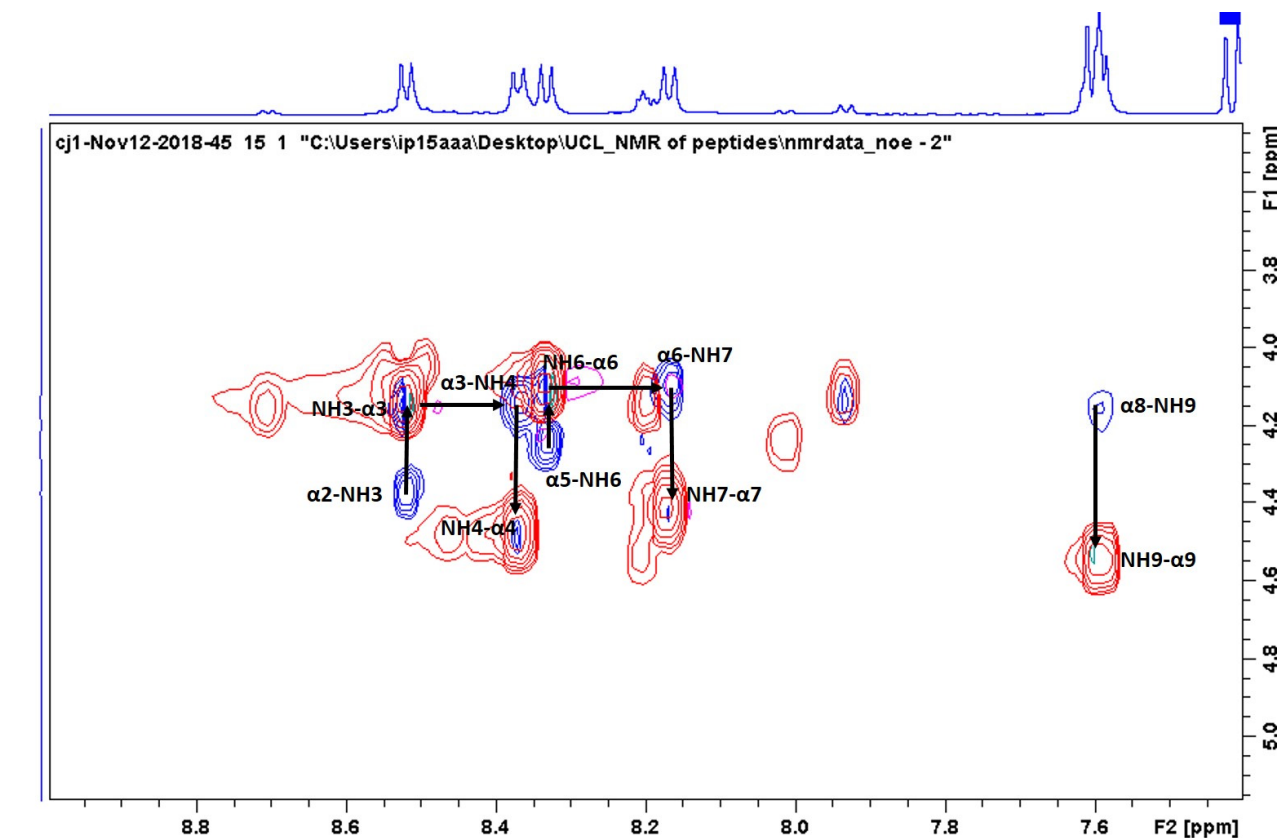


Figure S26. Overlay of the aromatic regions obtained from 2D ^1H - ^1H TOCSY (red) and NOESY (blue) NMR spectra of sample 27 (RPRRPRLPW), with the relevant connectivity indicated by black arrows.

Table S3. Assignment of ^1H NMR spectra of peptide 27 (RPRRPRLPW) based on the overlapping of TOCSY and NOESY experiments.

Residue	$\text{H-N}\alpha$	$\text{H-}\alpha$	$\text{H-}\beta$	$\text{H-}\gamma$	$\text{H-}\delta$	Other
Arg 1	Not visible					
Pro 2		4.37	2.25; 1.92	2.22; 1.77	3.66; 3.47	
Arg 3	8.52	4.14	1.67	1.54	2.88	
Arg 4	8.37	4.48	1.92	1.75	3.03	
Pro 5		4.24				
Arg 6	8.33	4.11	1.84	1.70	2.93	
Leu 7	8.17	4.42	1.47; 1.37	1.16	0.80; 0.76	
Pro 8		4.15				
Trp 9	7.59	4.52	2.96		6.92-7.40	Ar) 10.9 (N^αH)

4. Biological assays

Table S4. Minimum inhibitory concentration (MIC) of synthesised peptides and of reference antibiotics novobiocin and norfloxacin.

MIC ($\mu\text{g/mL}$)		<i>E. coli</i>	<i>S. aureus</i>
Compound	Sequence		
Novobiocin		32	4
Norfloxacin		0.062	2
1	FRW	>128	>128
2	FWR	>128	>128
3	WRW	>128	>128
4	WRWR	>128	>128
5	RWRW	>128	>128
6	WRWRW	64	64
7	FRF	>128	>128
8	FRFR	>128	>128
9	RFRF	>128	>128
10	FRFRF	>128	>128
11	RRFRF	>128	>128
12	WKW	>128	>128
13	WKWK	>128	>128
14	KWKW	>128	>128
15	WKWKW	>128	>128
16	FKF	>128	>128
17	FKFK	>128	>128
18	KFKF	>128	>128
19	FKFKF	>128	>128
20	WRRQRW	>128	>128
21	FRRQRF	>128	>128
22	RPRPRPL	>128	>128
23	RPWPPR	>128	>128
24	WKPLPPR	>128	>128
25	FKPLPPH	>128	>128
26	RPPWRPPW	>128	>128
27	RPRRPRLPW	128	>128

Table S5. Antimicrobial activity of norfloxacin in presence of peptides which showed some activity in potentiating novobiocin. Assays were performed at fixed concentration of 128 µg/mL against susceptible *E. coli* 10418 and multidrug resistant clinical isolate *E. coli* G69. Potentiation assay for norfloxacin was also performed in presence of 64 µg/mL of RND efflux pump inhibitor PAβN. All tests were repeated in duplicate.

Compound	Sequence	MIC of norfloxacin (µg/mL)		
		<i>E. coli</i> 10418	<i>E. coli</i> G69	
Norfloxacin		0.062	>128	
+128 µg/mL of peptide				
1	FRW	0.062	>128	
2	FWR	0.062	>128	
3	WRW	0.062	>128	
4	WRWR	0.062	>128	
5	RWRW	0.062	>128	
6	WRWRW	0.062	>128	
7	FRF	0.062	>128	
9	RFRF	0.062	>128	
12	WKW	0.062	>128	
15	WKWKW	0.125	>128	
16	FKF	0.062	>128	
20	WRRQRW	0.062	>128	
21	FRRQRF	0.062	>128	
22	RPRPRPL	0.062	>128	
23	RPWPPR	0.062	>128	
24	WKPLPPR	0.062	>128	
25	FKPLPPH	0.062	>128	
26	RPPWRPPW	0.62	>128	
27	RPRRPRLPW	0.062	>128	
PAβN‡		0.125	>128	

‡ The MIC of norfloxacin was also measured in combination with 64 µg/mL of the known efflux pump inhibitor PaβN but no potentiation was observed, so the assay was not repeated at lower concentrations.

5. MD simulation and docking studies.

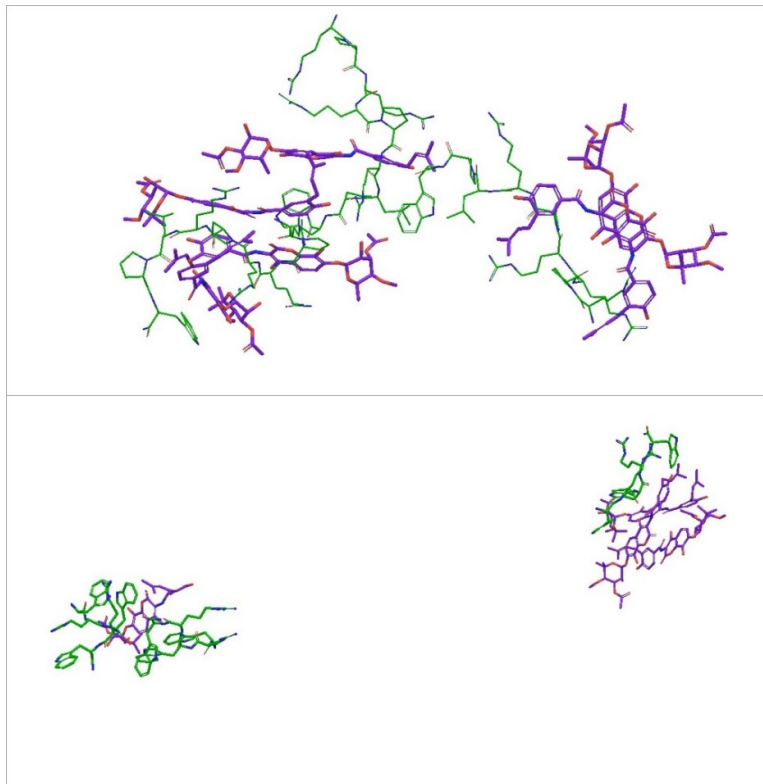


Figure S27. Top: the representative frame of the most populated cluster obtained from the trajectory of 50 ns MD simulation of a system containing peptide **27** (RPRRRPLPW-NH₂, green) and antibiotic novobiocin (purple). All molecules are involved in the formation of one major complex; Bottom: the representative frame of the most populated cluster obtained from the trajectory of 50 ns MD simulation of a system containing peptide **6** (WRWRW-NH₂, green) and novobiocin (purple). All molecules are involved in the formation of two complexes.

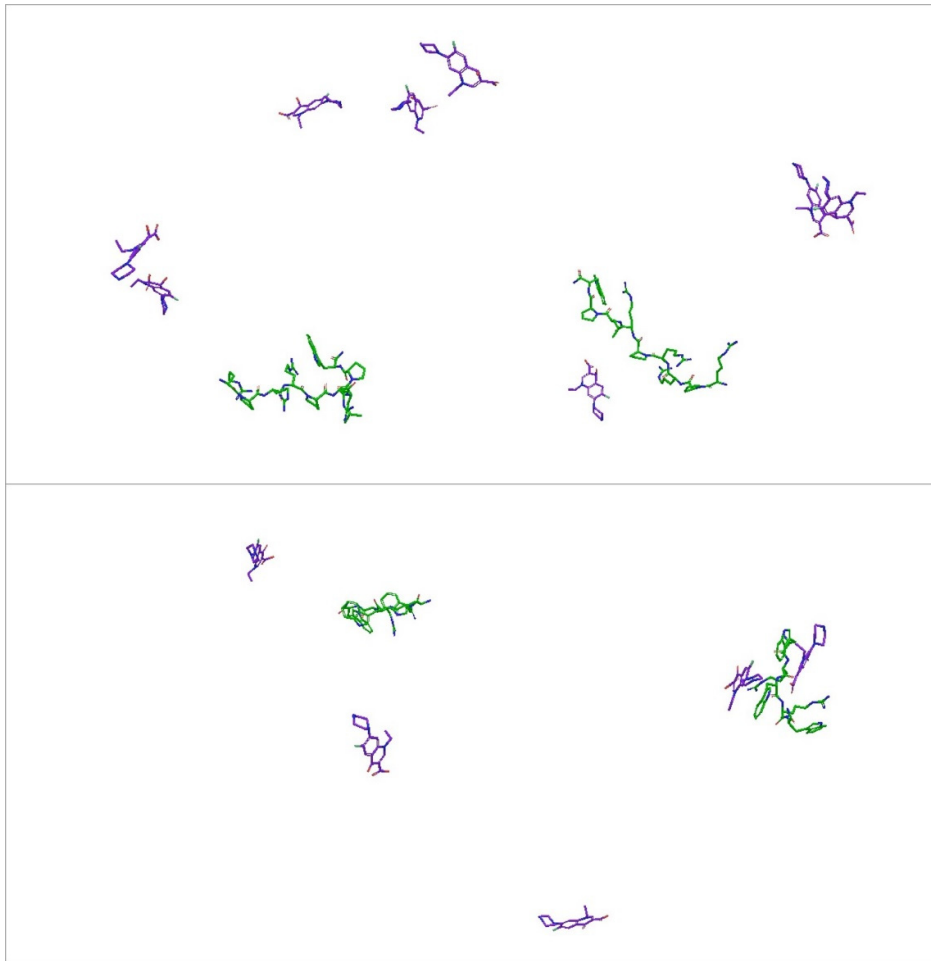


Figure S28. Top: representative frame of the most populated cluster obtained from the trajectory of 50 ns MD simulation of a system containing peptide **27** (RPRRRRLPW-NH₂, green) and antibiotic norfloxacin (purple). No complexes are formed. Bottom: representative frame of the most populated cluster obtained from the trajectory of 50 ns MD simulation of a system containing peptide **6** (WRWRW-NH₂, green) and norfloxacin (purple). Whilst the formation of a complex among two molecules of antibiotic and one of peptide can still be seen, the other three norfloxacin molecules are still scattered throughout the system.

6. Docking against RND efflux pump as a target

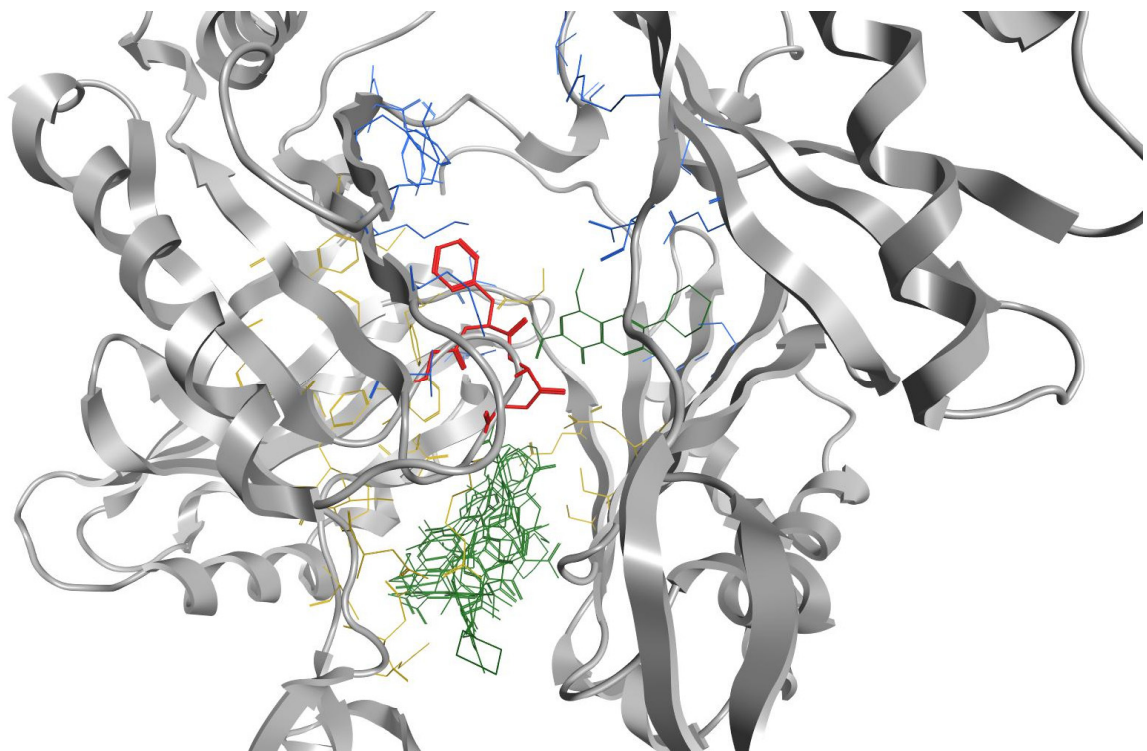


Figure S29. All poses of norfloxacin are found in the distal binding pocket (yellow sticks), with the exception of the most favourable one which is in the proximal binding pocket (blue sticks) instead, also establishing interaction with the glycine loop (red thick sticks).

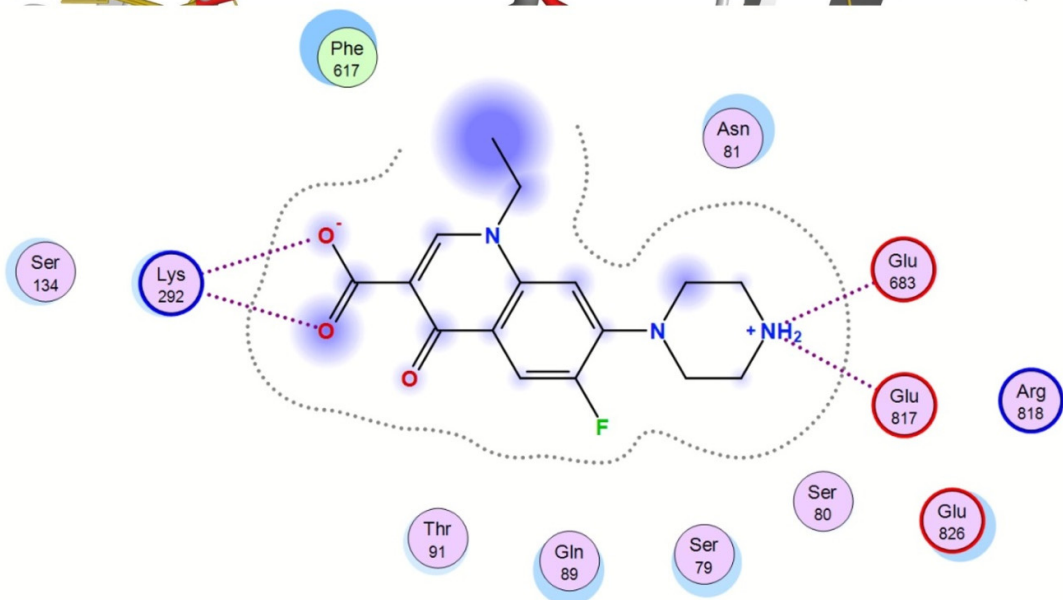
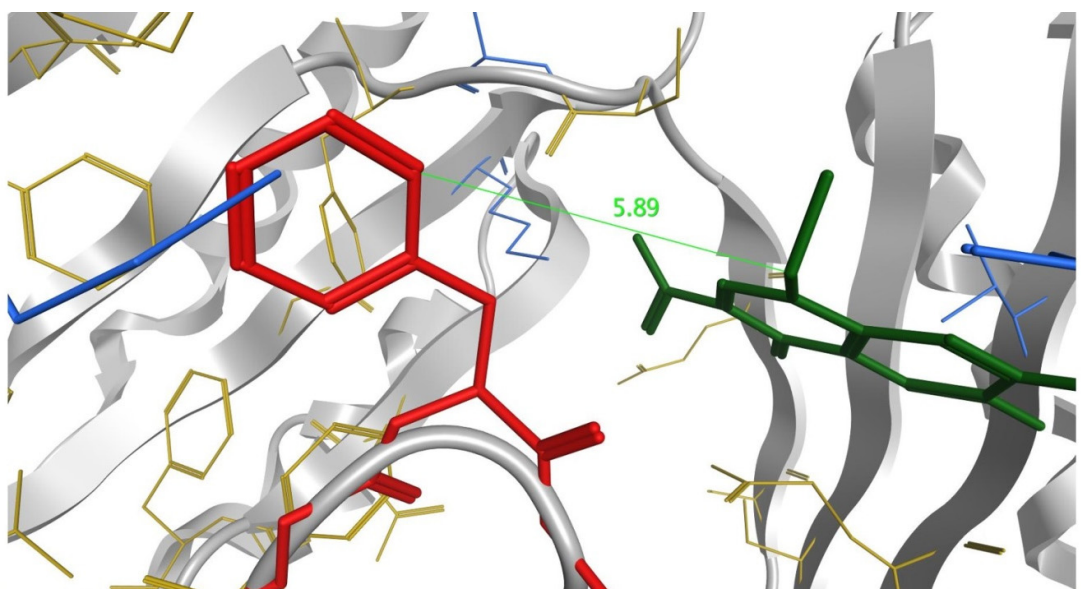


Figure S30. The most favourable pose of norfloxacin (green thick sticks) located in the proximal binding pocket (blue sticks) forms a hydrophobic interaction between C8 and the aromatic ring of Phe617.

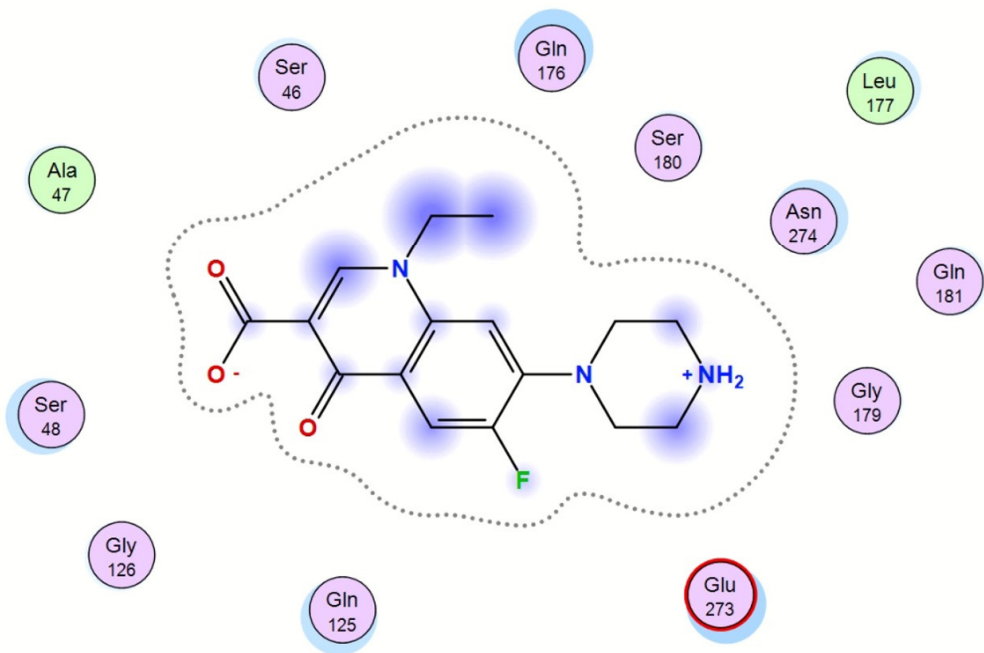
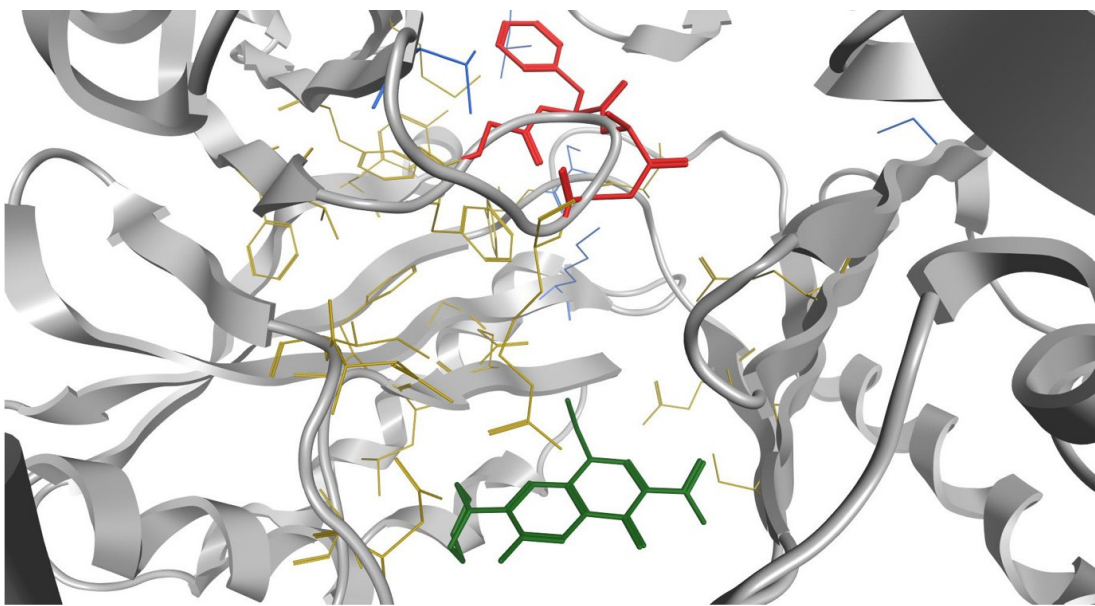


Figure S31. The second most favourable pose of norfloxacin (green thick sticks) located in the distal binding pocket (yellow sticks) established no interactions with the loop (red thick sticks).

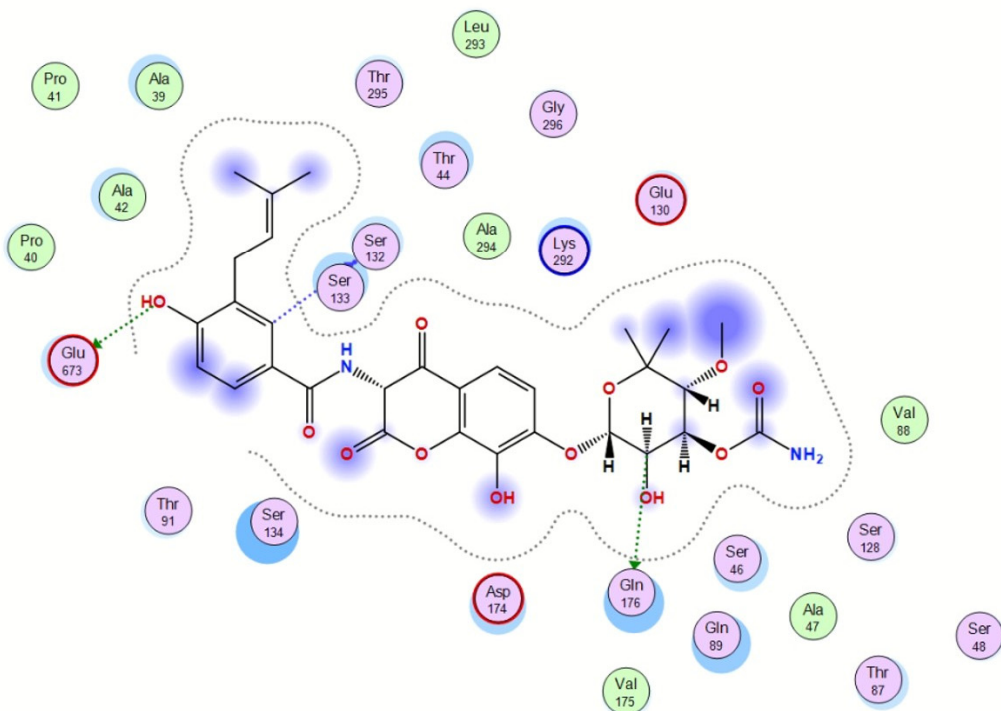
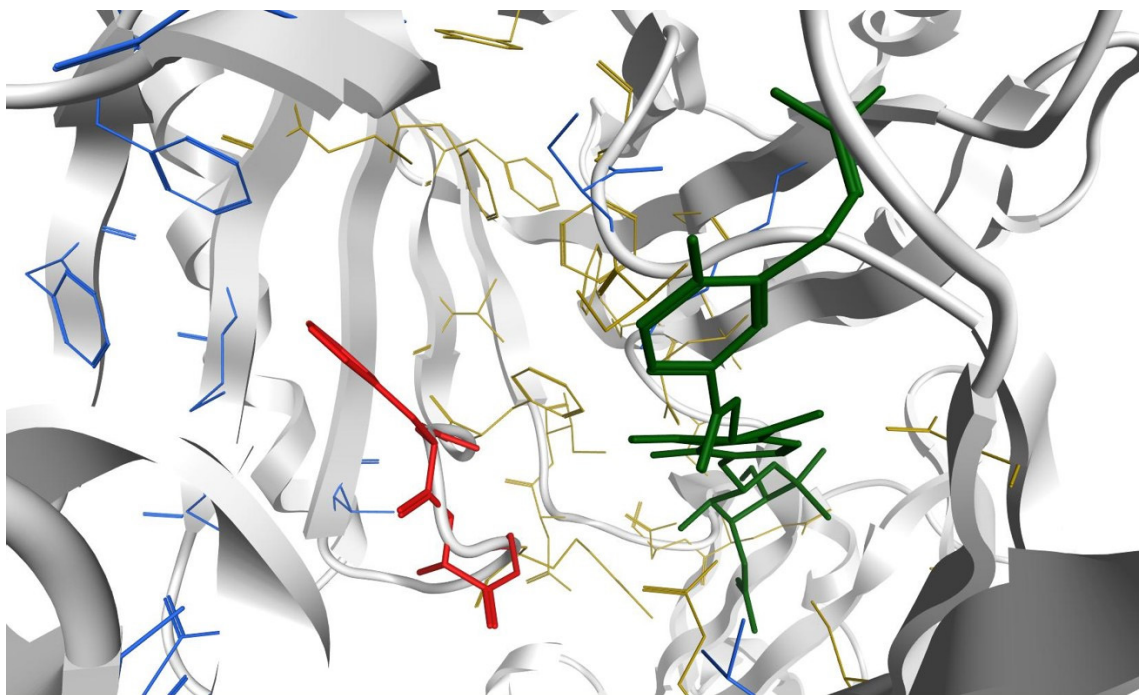


Figure S32. The most favourable pose of novobiocin (green thick sticks) located in the distal binding pocket (yellow sticks) does not interact with the loop (red thick sticks). The proximal binding pocket is shown in blue sticks.

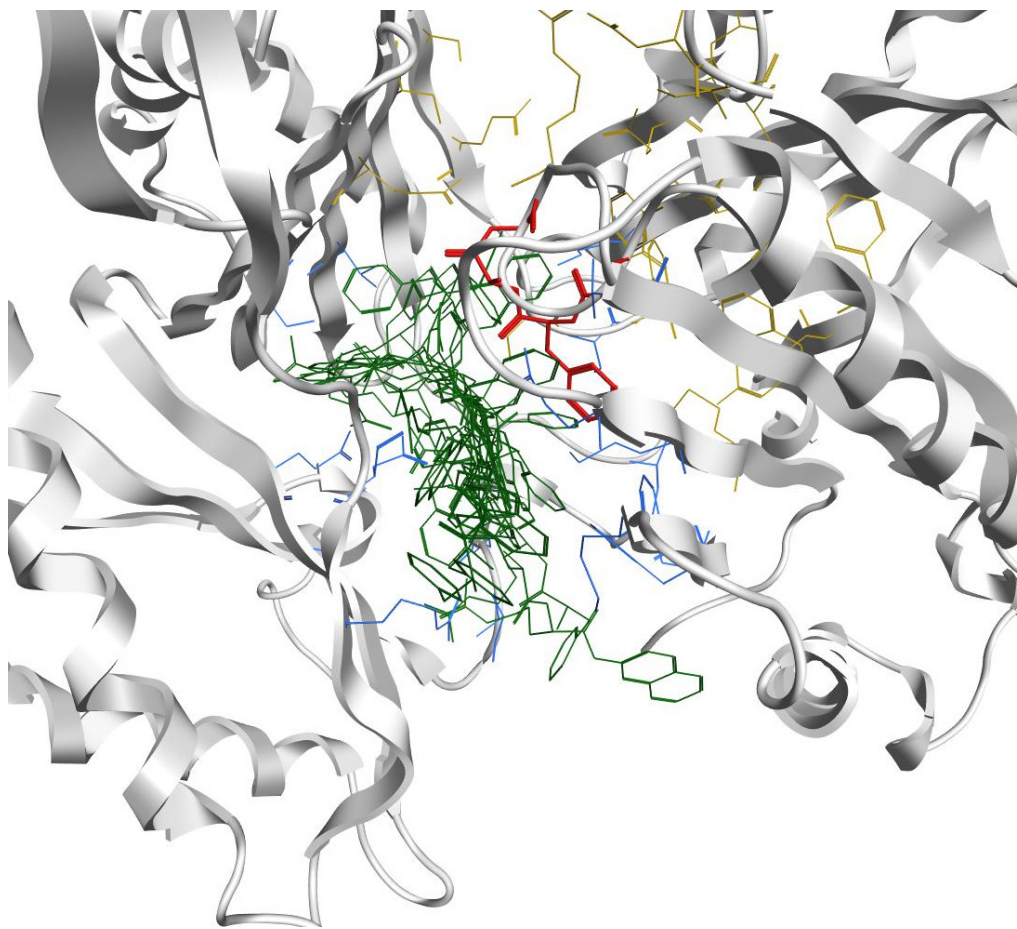


Figure S33. All 15 poses of PA β N (green stick representation) were found in the proximal binding pocket (blue sticks), with strong interactions with the glycine loop (red thick sticks) which regulates the passage of substrates between the proximal and distal pocket (yellow sticks). The distal binding pocket is shown in yellow sticks.

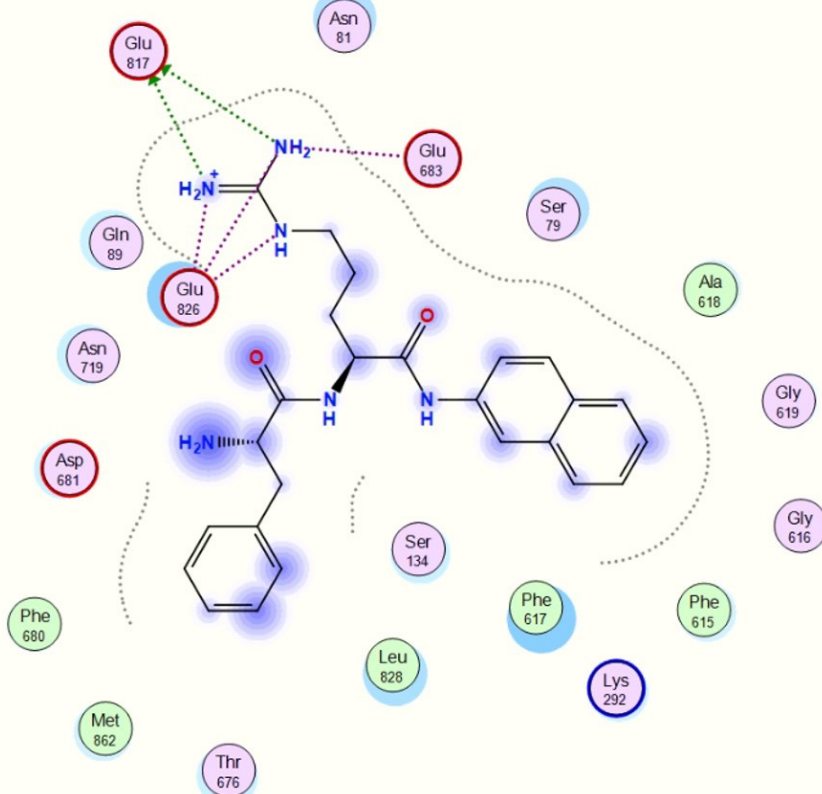
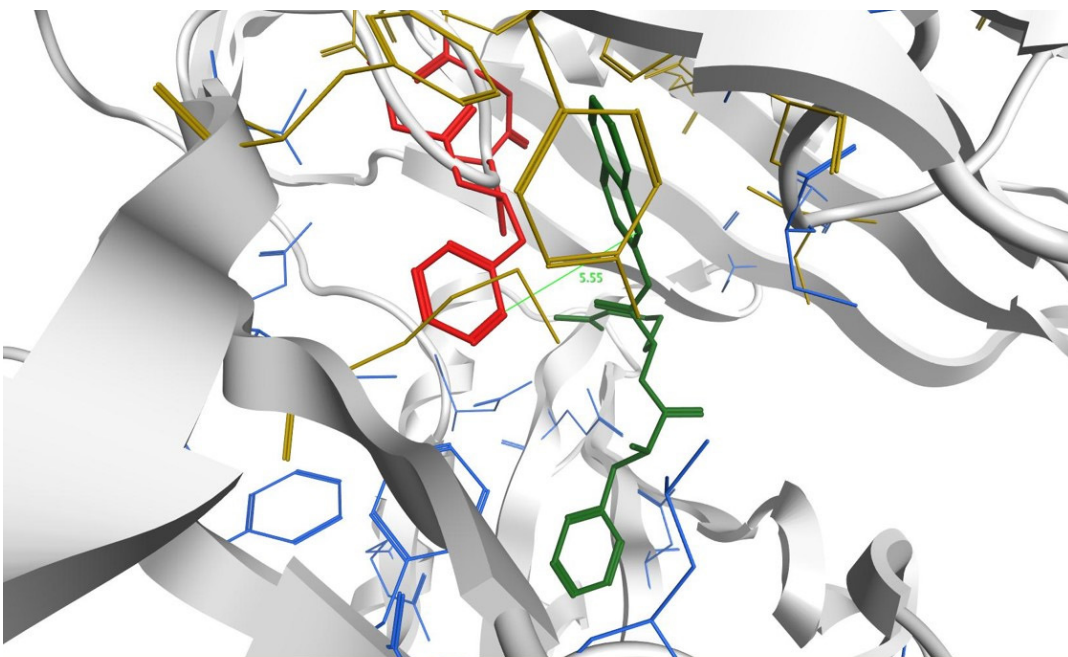


Figure S34. Most favourable pose of PA β N (green, thick lines representation) located in the periplasmic portion of the AcrB monomer of an E. Coli RND efflux pump (PDB ID 4DX5). An interaction can be seen with residues Phe617 and Ala618 which are part of the loop linking the distal and proximal binding pockets (pink, lines representation) and is thought to regulate passage of substrates through the pump.

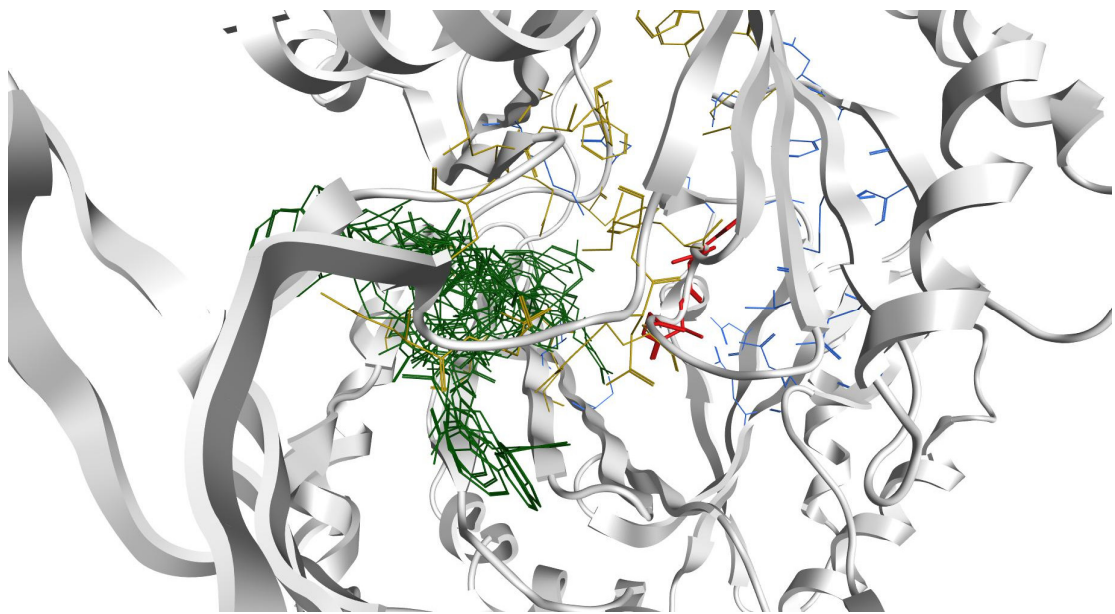


Figure S35. All poses of peptide 3 WRW (green sticks) located in the distal binding pocket (yellow sticks). The proximal binding pocket is shown as blue sticks and the loop as thick red sticks.

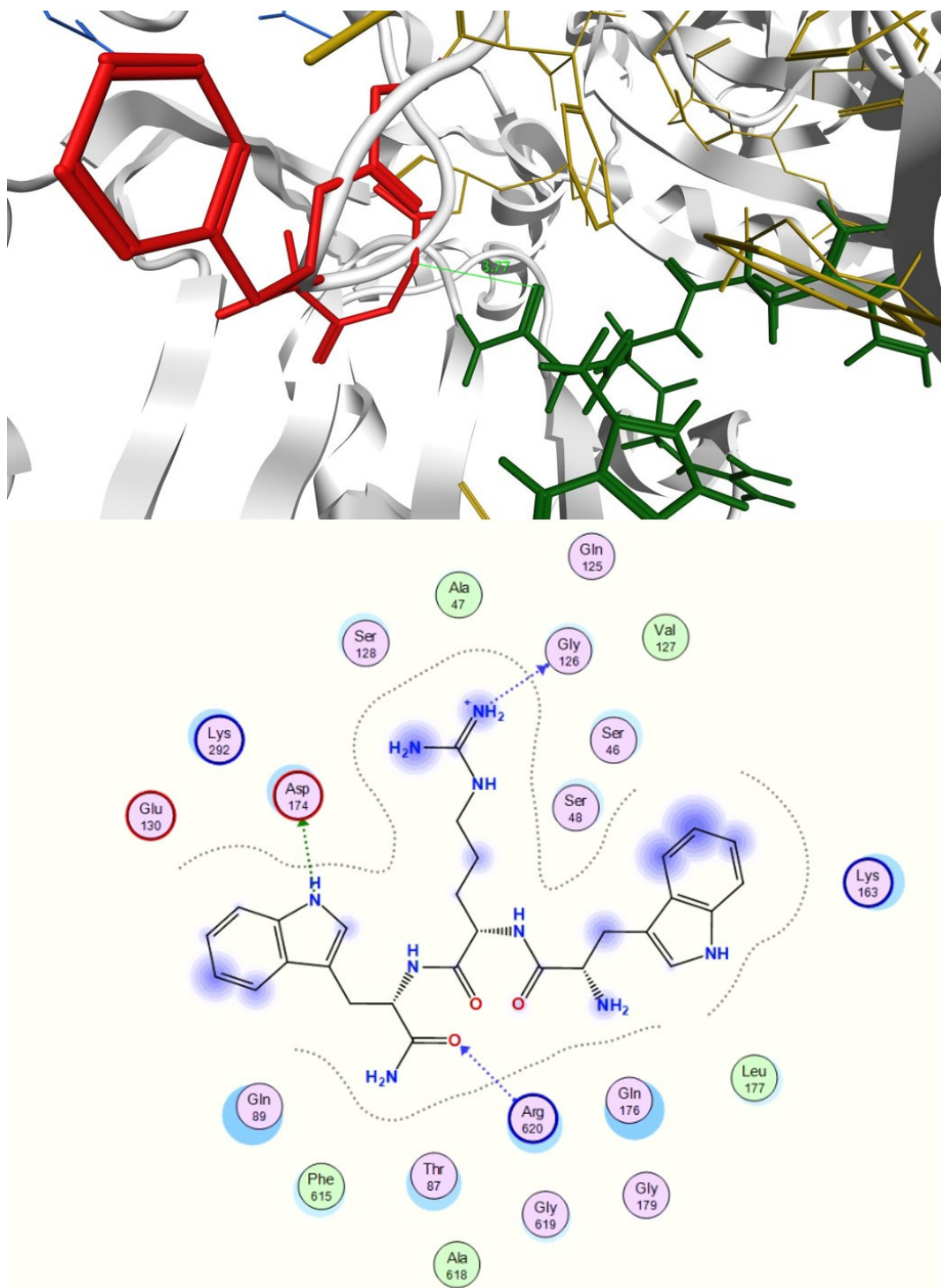


Figure S36. The most favourable pose of peptide 3 WRW (thick green sticks) located in the distal binding pocket (yellow sticks) shows an interaction with residues Ala618 and Gly619 of the loop (thick red sticks), but not with Phe617.

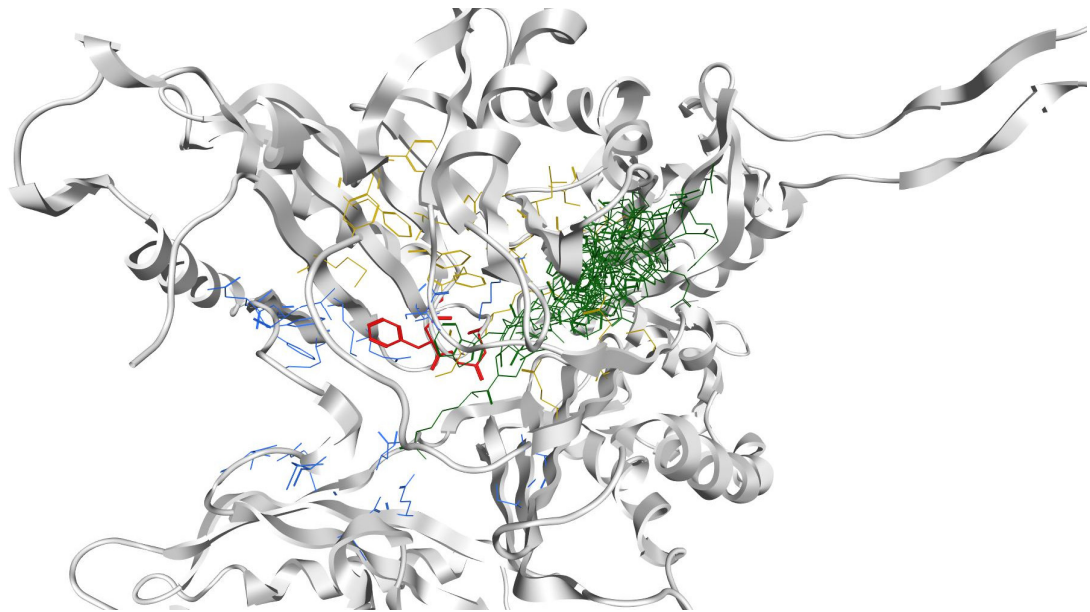


Figure S37. All poses of peptide **23** RPWPPR-NH₂ (green sticks), with the exception of the first two and the fourth, were found within the proximal distal binding pocket (yellow sticks) and no interactions were seen with the loop (thick red sticks).

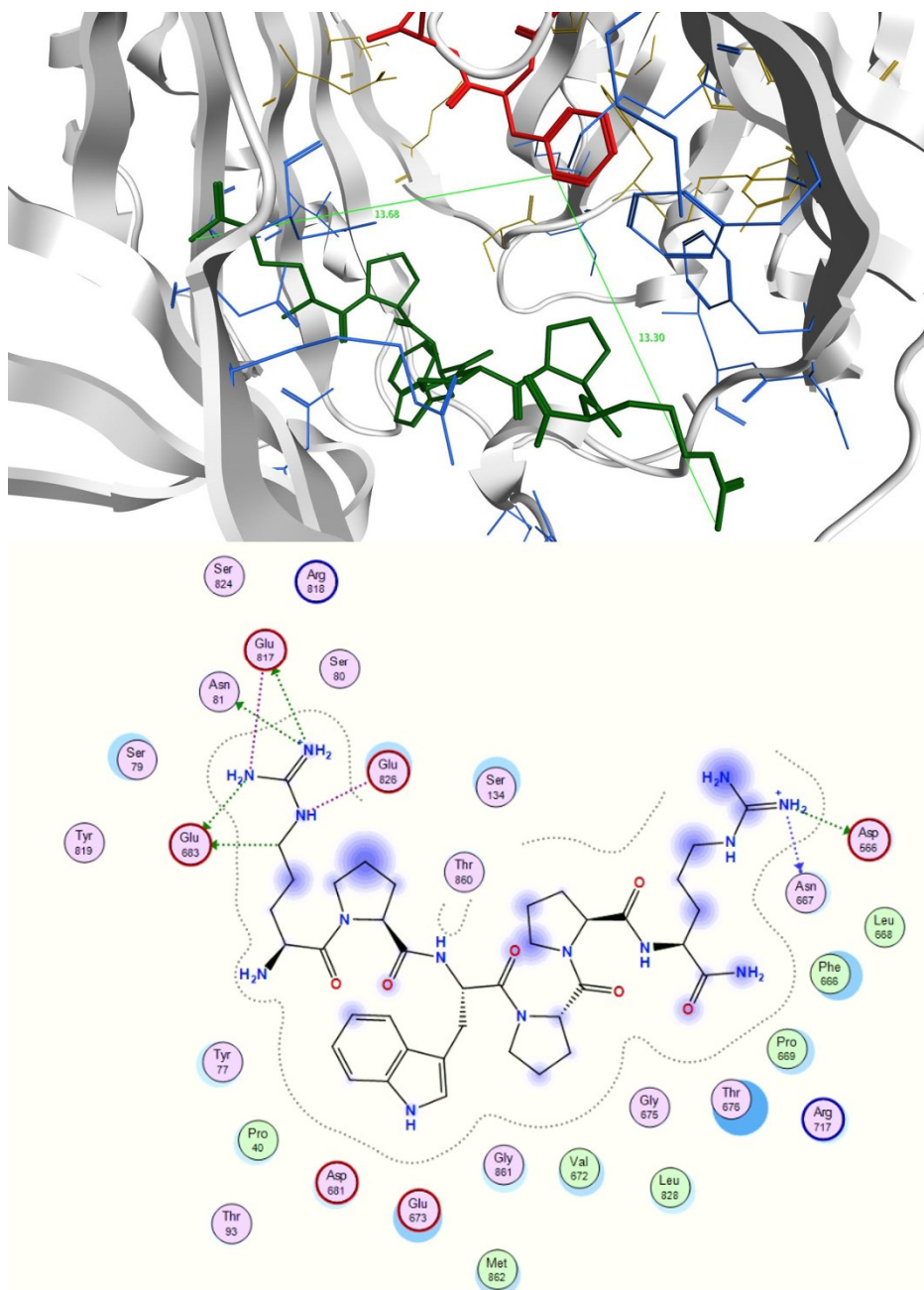


Figure S38. The most favourable pose of non potentiating peptide RPWPPR-NH₂ (green sticks) located in the proximal pocket (blue sticks) does not form interactions with the loop (thick red sticks). The distal pocket is shown as yellow sticks.